

ORIGINAL ARTICLE

Hyperbolic mixed-type inhibition of acetylcholinesterase by tetracyclic thienopyrimidines

C. M. González Tanarro & M. Gütschow

Pharmaceutical Institute, Pharmaceutical Chemistry I, University of Bonn, Bonn, Germany

Abstract

A series of tetracyclic thienopyrimidines (7–14) was prepared and investigated as inhibitors of acetylcholinesterase from *Electrophorus electricus* acetylcholinesterase (EeAChE), as well as human acetylcholinesterase (hAChE) and human butyrylcholinesterase (hBChE). A new synthetic procedure was employed for the synthesis of the angularly fused heterocycles 7–10. Among them, the presence of a tetrahydropyrido ring with a benzyl rest at the basic nitrogen was required for EeAChE inhibition. A detailed kinetic analysis of the hyperbolic mixed-type inhibition of EeAChE by 9–14 was performed. These heterocyclic compounds inhibited EeAChE with K_i values of less than 3 μM . Most values were relatively close to 1, indicating a similar affinity of the inhibitor to the free enzyme and the enzyme-substrate complex. Inhibitor 10 displayed a rather uncompetitive pattern of inhibition ($\alpha=0.47$) and a relatively high residual activity of a postulated ternary enzyme-substrate-inhibitor complex ($\beta=0.24$).

Keywords: Acetylcholinesterase, hyperbolic mixed-type inhibition, tetracyclic inhibitors.

Introduction

The serine hydrolase acetylcholinesterase (AChE), a member of the α/β hydrolase family hydrolyzes a broad range of ester and amide substrates, including the neurotransmitter acetylcholine (ACh)^{1,2}. Substrate cleavage proceeds through an acyl transfer mechanism and is mediated by the catalytic triad Ser200-His440-Glu327 (*Torpedo californica* AChE (TcAChE), numbering)³ located within the active-site at the bottom of a 20 Å deep gorge. Substrate binding is facilitated by the anionic site were aromatic residues, such as Trp84 and Phe330, interact *via* cation- π interactions and the acidic side chain of Glu199 *via* electrostatic interaction with the quaternary ammonium group of ACh or acetylthiocholine (ATCh)^{3,4}. A second substrate binding site, the peripheral anionic site (PAS), consists of five residues, Tyr70, Asp72, Tyr121, Trp279, and Tyr334, clustered around the entrance of the active-site gorge³⁻⁵. In addition to the principal physiological function of AChE, that is, hydrolysis of ACh at cholinergic synapses and neuromuscular junctions, several 'non-classical' activities of AChE are associated with the PAS^{2,5}. For example, AChE has been shown to

promote the aggregation and toxicity of β -amyloid, both *in vivo* and *in vitro*⁶.

It was proposed over 25 years ago that degeneration of cholinergic neurons in the basal forebrain and the associated loss of cholinergic neurotransmission in the cerebral cortex contributed significantly to the deterioration in cognitive function seen in patients with Alzheimer's disease (AD). This cholinergic hypothesis of AD has served as the basis for the majority of treatment strategies and drug development approaches for AD to date. The AChE inhibitors donepezil (Figure 1), galantamine, and rivastigmine are frequently used drugs to treat the symptoms of AD⁷⁻¹¹. Various carbamates have been characterized as pseudo-substrate inhibitors of AChE¹². During the last decade, several hybrid molecules derived from tacrine (Figure 1) and heterobivalent tacrine derivatives, simultaneously targeting both the active and the PAS, have been developed as inhibitors for both AChE and its relative butyrylcholinesterase (BChE)^{9-11,13-15}. For example, we have designed linker-connected dimers of tacrine with gallamine (Figure 1)¹⁶ or with a coumarin fluorophor¹⁷. The latter heterodimer was shown to act

Address for Correspondence: Michael Gütschow, Pharmaceutical Institute, Pharmaceutical Chemistry I, University of Bonn, An der Immenburg 4, D-53121 Bonn, Germany. Tel.: +49-228-73-2317. E-mail: guetschow@uni-bonn.de

(Received 19 May 2010; revised 23 June 2010; accepted 24 June 2010)

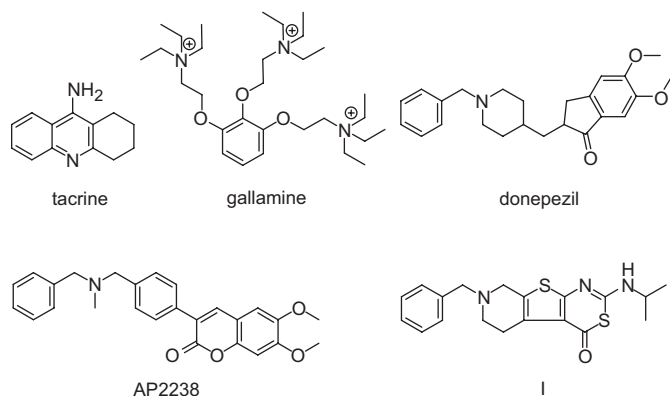


Figure 1. Inhibitors of acetylcholinesterase.

not only as an AChE inhibitor in sections from perfused wild-type and triple-transgenic mice, but also as a useful fluorescent probe for β -amyloid in tissues from triple-transgenic mice *in vitro*¹⁷ and *in vivo*¹⁸.

In a previous study, we described 7-benzyl-5,6,7,8-tetrahydro-2-isopropylamino-4*H*-pyrido[4',3':4,5]thieno[2,3-*d*][1,3]thiazin-4-one I (Figure 1) which inhibits AChE in the submicromolar range¹⁹. Kinetic analysis as well as structural similarities between donepezil²⁰, AP2238 (Figure 1)²¹, and I suggested that these substances act as dual site inhibitors of AChE and bind along the active-site gorge. A detailed kinetic study with compound I and the prototype inhibitors tacrine and gallamine was performed, and I was characterized as a hyperbolic mixed-type inhibitor of AChE from *Electrophorus electricus*²². A new series of heterocyclic compounds was designed on the basis of structure I as follows. Replacement of the thiazine ring sulfur by nitrogen allowed the fusion of a further ring to the resulting template, i.e. to the 7-benzyl-5,6,7,8-tetrahydro-pyrido[4',3':4,5]thieno[2,3-*d*]pyrimidin-4(1*H*)-one scaffold. This modification was realized in the tetracyclic representatives 9 and 10 (for structures, see Table 1). The same heterocyclic rings, i.e. imidazole and pyrimidine, were incorporated in the angularly fused structures 13 and 14. Replacement of the benzyl-substituted nitrogen by a methylene unit resulted in the tetrahydrobenzo analogs 7, 8, and 11, 12 respectively. These eight compounds were included in a kinetic study with AChE from *Electrophorus electricus* AChE (EeAChE). Their inhibitory activities toward human AChE (hAChE) and human BChE (hBChE) are also reported herein.

Materials and methods

General methods and materials

Melting points were obtained on a Rapido Boetius apparatus and are uncorrected. ¹H nuclear magnetic resonance (NMR) spectra (500 MHz) and ¹³C NMR spectra (125 MHz) were recorded on a Bruker Avance instrument. Elemental analyses were performed on a Vario EL apparatus. Thin-layer chromatography was carried out using aluminum sheets coated with silica gel 60 F₂₅₄

(Merck). Enzymatic activity of cholinesterases was measured at a Varian Cary Bio 50 UV/Vis spectrophotometer. AChE from EeAChE was purchased from Fluka (Deisenhofen, Germany). Human acetylcholinesterase (hAChE), ATCh, butyrylthiocholine (BTCh) and 5,5'-dithio-bis-(2-nitrobenzoic acid) (DTNB) were obtained from Sigma (Steinheim, Germany). hBChE was purchased from Lee Biosolutions (St. Louis, MO). Compounds 5 and 6 were prepared according to reported procedures²³⁻²⁶. Compounds 11-14 were synthesized according to literature reports^{27,28}.

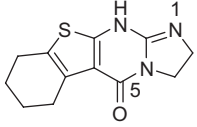
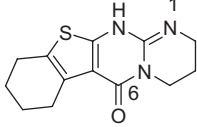
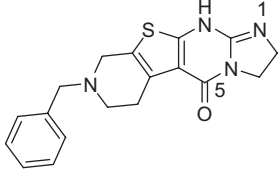
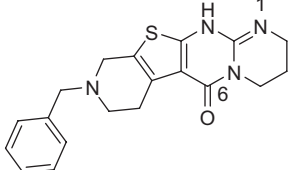
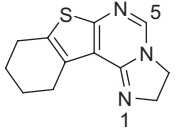
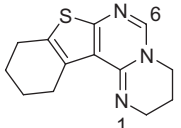
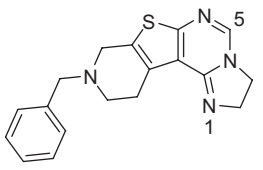
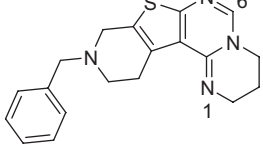
Synthesis

*2,3,6,7,8,9-Hexahydro-benzothieno[2,3-*d*]-imidazo[1,2-*a*]pyrimidin-5(1*H*)-one (7): general procedure for the preparation of linearly fused compounds 7-10.* To a solution of compound 5 (0.98 g, 3 mmol) in 2-methoxyethanol (12 mL), ethylenediamine (11.54 g, 12.8 mL, 192 mmol) was added. The mixture was stirred in a sealed flask at 150°C for 24 h. After it was cooled, the solution was poured onto ice-water (150 mL), and the precipitate was filtered off. The crude material was recrystallized from toluene to give 7 (0.69 g, 93%). An analytic sample was obtained from recrystallization from ethanol: mp 261-267°C, conversion 196-201°C; ¹H NMR [dimethyl sulfoxide *d*₆ (DMSO-*d*₆)] δ 1.68-1.78 (m, 4H, 7-H, 8-H), 2.57-2.60, 2.74-2.77 (each m, total 4H, 6-H, 9-H), 3.61, 4.01 (each t, *J* = 8.7 Hz, total 4H, 2-H, 3-H), 7.72 (s, 1H, 11-H); ¹³C NMR (DMSO-*d*₆) δ 22.06, 22.86 (C-7, C-8), 24.33, 25.38 (C-6, C-9) 40.06, 42.12 (C-2, C-3), 114.00 (C-5a), 125.15, 130.14 (C-5b, C-9a), 155.88, 157.00 (C-11a, C-10a), 166.02 (C-5). Anal. found: C, 58.74; H, 5.46; N, 16.50; S, 12.52. C₁₂H₁₃N₃OS requires: C, 58.28; H, 5.30; N, 16.99; S, 12.97.

*2,3,4,7,8,9,10,12-Octahydro-6*H*-benzothieno[2,3-*d*]pyrimido[1,2-*a*]pyrimidin-6-one (8).* A mixture of compound 5 (0.98 g, 3 mmol) and 1,3-diaminopropane (2.96 g, 3.4 mL, 40 mmol) was refluxed for 40 h. It was kept at 0°C for 48 h, the precipitate was filtered off and washed with H₂O. The crude product was dried and recrystallized from toluene to give 8 (0.46 g, 59%): mp 292-293°C; ¹H NMR (DMSO-*d*₆) δ 1.67-1.77 (m, 4H, 8-H, 9-H), 1.88-1.91 (m, 2H, 3-H), 2.55-2.57, 2.73-2.76 (each m, total 4H, 7-H, 10-H), 3.27-3.25, 3.84 (m, t, *J* = 5.8 Hz, total 4H, 2-H, 4-H), 7.71 (s, 1H, 12-H); ¹³C NMR (DMSO-*d*₆) δ 19.85 (C-3), 22.11, 22.90 (C-8, C-9), 24.33, 25.42 (C-7, C-10) 38.64, 38.82 (C-2, C-4), 112.23 (C-6a), 123.83, 130.21 (C-6b, C-10a), 150.02, 157.67 (C-11a, C-12a), 165.10 (C-6). Anal. found: C, 60.01; H, 6.10; N, 15.64; S, 11.90. C₁₃H₁₅N₃OS requires: C, 59.74; H, 5.79; N, 16.08, S, 12.27.

*8-Benzyl-2,3,6,7,8,9-hexahydro-imidazo[1,2-*a*]pyrido[4',3':4,5]thieno[2,3-*d*]pyrimidin-5(1*H*)-one (9).* Compound 6 (1.26 g, 3 mmol) was reacted with ethylenediamine (11.54 g, 12.8 mL, 192 mmol) in 2-methoxyethanol (12 mL). The crude product was recrystallized from 2-methoxyethanol to give 9 (0.38 g, 38%): mp 222-225°C; ¹H NMR (DMSO-*d*₆) δ 2.70 (t, *J* = 5.7 Hz, 2H, 7-H), 2.82 (t, *J* = 5.7 Hz, 2H, 6-H), 3.45 (s, 2H, 9-H), 3.62, 4.00 (each t, *J* = 8.8 Hz, total 4H, 2-H, 3-H), 3.65 (s,

Table 1 Inhibition of acetylcholinesterase from *Electrophorus electricus* (EeAChE), human acetylcholinesterase (hAChE) and human butyrylcholinesterase (hBChE) by compounds 7-14.

Compound	EeAChE				hAChE	hBChE
	IC ₅₀ ^a ± SEM (μM)	K _i ± SEM (μM)	αK _i ± SEM (μM)	β ± SEM	IC ₅₀ ^a ± SEM (μM)	IC ₅₀ ^b ± SEM (μM)
7 	> 75	nd ^c	nd	nd	> 200	> 200
8 	> 75	nd	nd	nd	> 200	> 200
9 	1.35 ± 0.06	1.55 ± 0.09	1.08 ± 0.03	0.084 ± 0.001	14.2 ± 0.3	> 200
10 	1.51 ± 0.07	2.07 ± 0.19	0.98 ± 0.13	0.24 ± 0.02	5.69 ± 0.55	51.5 ± 10.2
11 	1.75 ± 0.10	1.32 ± 0.08	2.70 ± 0.59	0.14 ± 0.01	56.0 ± 4.5	88.0 ± 1.0
12 	2.26 ± 0.15	1.92 ± 0.12	2.87 ± 0.20	0.17 ± 0.01	20.5 ± 1.9	131 ± 7
13 	3.09 ± 0.25	2.36 ± 0.22	3.88 ± 0.22	0.16 ± 0.01	21.8 ± 1.6	89.9 ± 3.7
14 	1.73 ± 0.10	1.50 ± 0.07	2.34 ± 0.17	0.12 ± 0.004	62.5 ± 6.0	119 ± 14

^aIC₅₀ values with standard error were calculated from duplicate experiments at five inhibitor concentrations at a substrate concentration [acetylthiocholine] = 500 μM. Data were fitted to Equation 1. Limits were calculated from duplicate inhibition experiments at a single inhibitor concentration.

^bIC₅₀ values with standard error were calculated from duplicate experiments at five inhibitor concentrations at a substrate concentration [butyrylthiocholine] = 500 μM. Data were fitted to the equation of a competitive inhibition (Equation 5). Limits were calculated from duplicate inhibition experiments at a single inhibitor concentration.

^cnd, not determined.

2H, C₆H₅-CH₂), 7.23-7.34 (m, 5H, C₆H₅), 7.80 (s, 1H, 11-H);
¹³C NMR (DMSO-*d*₆) δ 25.74 (C-6), 40.08, 42.10 (C-2, C-3),
 49.35 (C-7), 51.00 (C-9), 61.11 (C₆H₅-CH₂), 113.60 (C-5a),
 122.85, 128.54 (C-5b, C-9a), 127.15 (C-4'), 128.37, 128.89
 (C-2', C-3'), 138.38 (C-1'), 156.02, 156.93 (C-10a, C-11a),

166.50 (C-5). Anal. found: C, 64.20; H, 5.89; N, 16.43.
 C₁₈H₁₈N₄OS requires: C, 63.88; H, 5.36; N, 16.56.

9-Benzyl-2,3,4,7,8,9,10,12-octahydro-6H-pyrido[4',3':4,5]thieno[2,3-d]pyrimido[1,2-a]pyrimidin-6-one (10). Compound 6 (1.26 g, 3 mmol) was reacted

with 1,3-diaminopropane (14.23 g, 16 mL, 192 mmol) in 2-methoxyethanol (12 mL). The crude product was recrystallized from 2-methoxyethanol to give 10 (125 mg, 11%): mp 202–207°C, conversion 193–197°C; ¹H NMR (DMSO-*d*₆) δ 1.88–1.93 (m, 2H, 3-H), 2.70 (t, *J*=5.7 Hz, 2H, 8-H), 2.79–2.81 (m, 2H, 7-H), 3.44 (s, 2H, 10-H), 3.65 (s, 2H, C₆H₅-CH₂), 3.84 (t, *J*=5.8 Hz, 2H, 2-H or 4-H), 7.30–7.33 (m, 5H, C₆H₅), 7.76 (s, 1H, 12-H), one signal (2H, 2-H or 4-H) is not visible due to the water signal (3.20–3.40); ¹H NMR (CDCl₃) δ 2.02–2.07 (m, 2H, 3-H), 2.83 (t, *J*=5.8 Hz, 2H, 8-H), 3.03 (t, *J*=5.8 Hz, 2H, 7-H), 3.44–3.48, 4.01 (m, t, *J*=5.8 Hz, total 4H, 2-H, 4-H), 3.55 (s, 2H, 10-H), 3.72 (s, 2H, C₆H₅-CH₂), 6.42 (s, 1H, 12-H), 7.27–7.37 (m, 5H, C₆H₅); ¹³C NMR (DMSO-*d*₆) δ 19.79 (C-3), 25.80 (C-7), 38.63, 38.84 (C-2, C-4), 49.39, 51.06 (C-8, C-10), 61.13 (C₆H₅-CH₂), 111.76 (C-6a), 121.47, 128.64 (C-6b, C-10a), 127.15 (C-4'), 128.37, 128.90 (C-2', C-3'), 138.42 (C-1'), 150.91, 157.68 (C-11a, C-12a), 165.77 (C-6). Anal. found: C, 61.99; H, 5.66; N, 15.03. C₁₉H₂₀N₄OS × H₂O requires: C, 61.60; H, 5.99; N, 15.12.

*2,3,8,9,10,11-Hexahydro-benzothieno[3,2-*e*]imidazo[1,2-*c*]pyrimidine* (11). ¹H NMR (DMSO-*d*₆) δ 1.67–1.80 (m, 4H, 9-H, 10-H), 2.65–2.69, 2.74–2.78 (each m, total 4H, 8-H, 11-H), 3.83 (t, *J*=9.9 Hz, 2H, 2-H), 4.00 (t, *J*=9.9 Hz, 2H, 3-H), 7.90 (s, 1H, 5-H). ¹³C NMR (DMSO-*d*₆) δ 22.01, 22.70 (C-9, C-10), 24.49, 25.44 (C-8, C-11), 45.27 (C-3), 53.17 (C-2), 117.22 (C-11b), 130.47, 131.36 (C-7a, C-11a), 144.20 (C-5), 150.70, 157.56 (C-6a, C-11c).

*3,4,9,10,11,12-Hexahydro-2H-benzothieno[3,2-*e*]pyrimido[1,2-*c*]pyrimidine* (12). ¹H NMR (DMSO-*d*₆) δ 1.67–1.77 (m, 4H, 10-H, 11-H), 1.86–1.92 (m, 2H, 3-H), 2.67–2.72, 2.84–2.88 (each m, total 4H, 9-H, 12-H), 3.43 (t, *J*=5.7 Hz, 2H, 2-H), 3.95 (t, *J*=5.4 Hz, 2H, 4-H), 7.73 (s, 1H, 6-H); ¹H NMR (CDCl₃) δ 1.69–1.78 (m, 4H, 10-H, 11-H), 1.89–1.94 (m, 2H, 3-H), 2.64–2.67, 2.87–2.90 (each m, total 4H, 9-H, 12-H), 3.51 (t, *J*=5.7 Hz, 2H, 2-H), 3.77 (t, *J*=5.8 Hz, 2H, 4-H), 7.16 (s, 1H, 6-H); ¹³C NMR (DMSO-*d*₆) δ 19.59 (C-3), 22.08, 22.40 (C-10, C-11), 24.87, 26.60 (C-9, C-12), 43.04 (C-2), 46.47 (C-4), 120.05 (C-12b), 130.84, 132.27 (C-8a, C-12a), 144.70, 155.87 (C-7a, C-12c), 146.81 (C-6).

*9-Benzyl-2,3,8,9,10,11-hexahydro-imidazo[1,2-*c*]pyrido[4',3':4,5]thieno[3,2-*e*]pyrimidine* (13). ¹H NMR (DMSO-*d*₆) δ 2.72 (t, *J*=5.8 Hz, 2H, 10-H), 2.82 (t, *J*=5.8 Hz, 2H, 11-H), 3.55 (s, 2H, 8-H), 3.67 (s, 2H, C₆H₅-CH₂), 3.85 (t, *J*=10.0 Hz, 2H, 2-H), 4.00 (t, *J*=10.0 Hz, 2H, 3-H), 7.23–7.35 (m, 5H, C₆H₅), 7.92 (s, 1H, 5-H); ¹³C NMR (DMSO-*d*₆) δ 25.67 (C-11), 45.33 (C-3), 49.23 (C-10), 51.06 (C-8), 53.18 (C-2), 60.9 (C₆H₅-CH₂), 116.79 (C-11b), 127.19 (C-4'), 128.39, 128.91 (C-2', C-3'), 128.85, 129.14 (C-7a, C-11a), 138.29 (C-1'), 144.46 (C-5), 150.57, 158.20 (C-6a, C-11c).

*10-Benzyl-3,4,9,10,11,12-hexahydro-2H-pyrido[4',3':4,5]thieno[3,2-*e*]pyrimido[1,2-*c*]pyrimidine* (14). ¹H NMR (DMSO-*d*₆) δ 1.80–1.85 (m, 2H, 3-H), 2.68 (t, *J*=5.8 Hz, 2H, 11-H), 2.89 (t, *J*=5.8 Hz, 2H, 12-H), 3.39 (t, *J*=5.5 Hz, 2H, 2-H), 3.52 (s, 2H, 9-H), 3.65 (s, 2H, C₆H₅-CH₂), 3.86 (t, *J*=5.7 Hz, 2H, 4-H), 7.13–7.33 (m, 5H, C₆H₅),

7.55 (s, 1H, 6-H); ¹³C NMR (DMSO-*d*₆) δ 20.13 (C-3), 27.11 (C-12), 43.79 (C-2), 46.07 (C-4), 49.51 (C-11), 51.30 (C-9), 60.96 (C₆H₅-CH₂), 120.98 (C-12b), 127.14 (C-4'), 128.37, 128.84 (C-2', C-3'), 128.62, 129.86 (C-8a, C-12a), 138.34 (C-1'), 143.44, 154.77 (C-7a, C-12c), 147.37 (C-6).

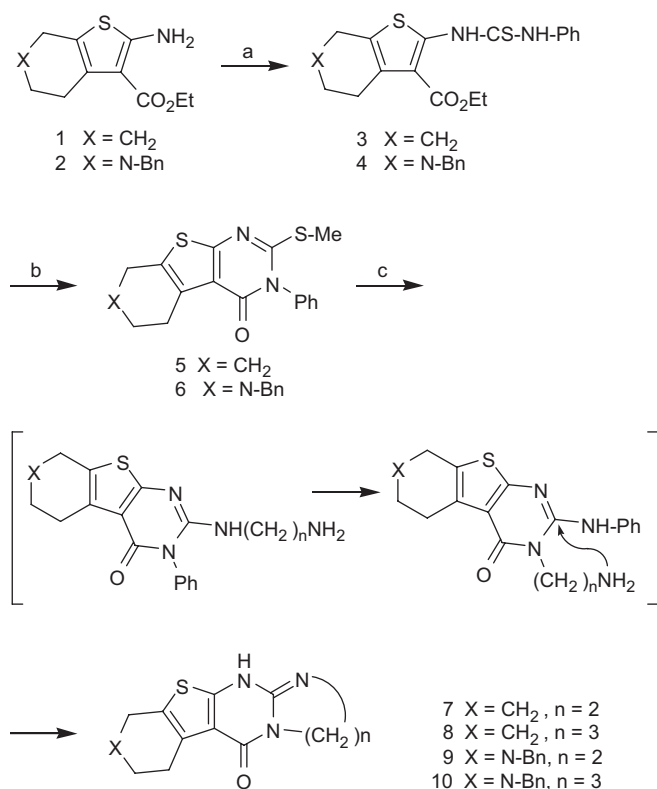
Enzyme inhibition experiments

Cholinesterase inhibition was assayed spectrophotometrically at 412 nm at 25°C^{19,29}. Product formation was monitored over 5 min. Assay buffer was 100 mM sodium phosphate, 100 mM NaCl, pH 7.3. Enzyme stock solutions were prepared with assay buffer in the following concentrations ~ 100 U/mL (EeAChE), ~ 3 U/mL (hAChE), ~ 10 U/mL (hBChE), and were kept at 0°C. Appropriate dilutions of the EeAChE (1:30) and hBChE (1:10) solutions were done immediately before starting the measurements. Solutions of ATCh (5, 10, 15, or 20 mM), BTCh (10 mM), and DTNB (7 mM) were prepared in assay buffer and kept at 0°C. Stock solutions of the inhibitors were prepared in acetonitrile. EeAChE was assayed as follows. Into a cuvette containing 830 μL assay buffer, 50 μL of the DTNB solution, 50 μL acetonitrile, 10 μL of an inhibitor solution, and 10 μL of an enzyme solution were added and thoroughly mixed. After incubation for 15 min at 25°C, the reaction was initiated by adding 50 μL of the ATCh solution. The following final concentration were used, ~ 0.033 U/mL of EeAChE, 250, 500, 750, or 1000 μM of ATCh, 350 μM of DTNB, 6% acetonitrile. Similarly, hAChE (final concentration ~ 0.03 U/mL) was assayed with 500 μM ATCh, and hBChE (final concentration ~ 0.01 U/mL) with 500 μM BTCh. The rates of enzyme-catalyzed substrate hydrolysis were corrected by those of the non-enzymatic hydrolysis of ATCh or BTCh, respectively, as determined by using 10 μL of assay buffer, instead of the enzyme solution. A *K*_m value of 550 μM¹⁹ for the substrate ATCh used in the EeAChE assay was taken for kinetic analyses.

Results and discussion

Synthesis

The preparation of the linearly fused compounds 7–10 is depicted in Scheme 1. Ethyl 2-aminothiophenecarboxylates 1 and 2 were prepared by Gewald synthesis, for a review, see³⁰, and reacted with phenylisothiocyanate to afford thiourea derivatives 3 and 4. Cyclocondensation and immediate S-alkylation³¹ gave tricyclic pyrimidines 5 and 6 bearing a nucleofuge at C-2. Indeed, upon reaction with diaminoalkanes, methylmercaptane was eliminated. The products, however, were formed by a more complex mechanism, which can be envisaged as follows. After the initial nucleophilic attack of the diaminoalkane and repulsion of the leaving group, a Dimroth rearrangement occurred. Then, an intramolecular nucleophilic attack of the terminal amino function, again at C-2, led to the replacement of aniline and formation of the fourth fused ring in the imidazo or pyrim-



Scheme 1. Synthesis of compounds 7–10. Reagents and conditions: (a) PhNCS, ethanol 80°C, 7h; (a) 1. 1N NaOH, EtOH, 2. MeI, room temperature; (c) ethylenediamine or 1,3-diaminopropane, 2-methoxyethanol, 150°C, 24h.

ido compounds 7–10. Their structures were confirmed by elemental analyses, ¹H and ¹³C NMR data. The angularly fused compounds 11–14 (structures in Table 1) were prepared according to literature reports^{27,28}, and NMR data, not published so far, are given in the Material and Methods section. NMR signals were assigned on the basis of and ¹H nuclear Overhauser effect and ¹³C/¹H correlation experiments. In order to distinguish the triplets for 2-H and 3-H (in the case of 11 and 13), or 2-H and 4-H (in the case of 12 and 14), respectively, a nuclear overhauser effect (NOE) experiment was exemplary done for compound 12 (Figure 2). On irradiation of the 6-H resonance, a NOE in 4-H was observed. The corresponding signals in the ¹³C NMR spectra were assigned with heteronuclear single-quantum coherence spectra.

Inhibition of cholinesterases

The activity of EeAChE was determined in a coupled assay with the substrate ATCh and DTNB. Active inhibitors were measured at five different concentrations. Plots of the rates versus inhibitor concentration, [I], did not become asymptotic to the x-axis. A residual activity at infinite concentration of the inhibitor, $v_{[I] \rightarrow \infty}$, was considered. The value of $v_{[I] \rightarrow \infty}$ at a defined substrate concentration was obtained from a plot of the rates versus [I] and non-linear regression according to Equation 1,

$$v = \frac{(v_0 - v_{[I] \rightarrow \infty})}{\left(1 + \frac{[I]}{IC_{50}}\right)} + v_{[I] \rightarrow \infty} \quad (1)$$

where v_0 is the velocity in the absence of the inhibitor. The IC_{50} value calculated by this equation corresponds to the concentration of the inhibitor which reduces the rate of the enzyme-catalyzed reaction to a velocity $(v_0 - v_{[I] \rightarrow \infty})/2 + v_{[I] \rightarrow \infty}$. Data from EeAChE inhibition experiments at a substrate concentration of 500 μM are given in Table 1. A corresponding plot for inhibitor 10 is shown in Figure 4B.

In order to discover the type of inhibition of compounds 9–14 towards EeAChE, the assay used to determine IC_{50} values was performed at four different substrate concentrations (250 μM, 500 μM, 750 μM, and 1000 μM). A general kinetic model (Figure 3) for the interaction with EeAChE was considered to account for the residual activity observed. This model includes the possible binding of the substrate, S, and the inhibitor, I, to the enzyme, E, at different sites and thus the formation of a ternary enzyme-substrate-inhibitor complex (ESI). The dissociation constants of ESI, are αK_S and αK_I . The complex ESI is still functional with a decreased rate of product formation governed by the catalytic constant, βk_p . This type of inhibition was referred to as hyperbolic mixed-type inhibition³².

To characterize the EeAChE-inhibitor interaction, the parameters α and β were determined by using the specific velocity plot, introduced by Baici³³. The kinetic analysis is exemplarily shown for inhibitor 10 in Figures 5 and 6. The specific velocity plot (Figure 5) is described by the specific velocity equation (Equation 2).

$$\frac{v_0}{v} = \frac{[I] \left(\frac{1}{\alpha K_i} - \frac{1}{K_i} \right) \frac{[S]}{K_m} + \left(1 + \frac{1}{K_i} \right)}{\left(1 + \beta \frac{[I]}{\alpha K_i} \right) \left(1 + \frac{[S]}{K_m} \right) \left(1 + \beta \frac{[I]}{\alpha K_i} \right)} \quad (2)$$

For the replots (Figure 6), the intersection points for $([S]/K_m)/(1 + [S]/K_m) = 0$ (a values) and for $([S]/K_m)/(1 + [S]/K_m) = 1$ (b values) were used. These replots according to Equations 3 and 4 gave β -values from the vertical intercept (Equation 4), and α -values from β and the vertical intercept (Equation 3). The plot according to Equation 3 gave access to the K_i value by dividing the slope by the intercept. The data for compounds 9–14 are given in Table 1.

$$\frac{a}{a-1} = \frac{\alpha K_i}{\alpha - \beta} \frac{1}{[I]} + \frac{\alpha}{\alpha - \beta} \quad (3)$$

$$\frac{b}{b-1} = \frac{\alpha K_i}{1 - \beta} \frac{1}{[I]} + \frac{1}{1 - \beta} \quad (4)$$

hAChE was assayed as described above for EeAChE, and IC_{50} values were obtained using Equation 1 (Table 1). The activity of hBChE was measured similarly with BTCh as the substrate. IC_{50} values were assigned by non-linear regression according to Equation 5.

$$v = \frac{v_0}{\left(1 + \frac{[I]}{IC_{50}}\right)} \quad (5)$$

As noted above, active EeAChE inhibitors of the present series exhibited residual activity at infinite concentration. This behavior is exemplarily shown for 10 in Figures 4A, 4B, 4C, and 4D, and the rates $v_{[I] \rightarrow \infty}$, relative to v_0 , are listed there. These findings let us conclude that β (Figure 3) takes a value different from zero. To elucidate the interaction between 9 and 14 and EeAChE, it was determined whether the inhibitor binds to the enzyme-substrate complex, ES, with a greater affinity than to the free enzyme, E, or *vice versa*. The preference of the inhibitor to bind to ES is reflected in values $\alpha < 1$ (Figure 3) that indicates mixed-type inhibition with a pronounced uncompetitive component. A higher affinity of the inhibitor to E, and thus values $\alpha > 1$, corresponds to mixed-type inhibition with a more competitive character. K_i values being independent of the substrate concentration also become available that way.

As shown in Figures 4A, 4B, 4C, and 4D, the $v_{[I] \rightarrow \infty}$ values of compound 10 (between 5% and 20%) increased with increasing substrate concentrations (between 250 and 1000 μM). This relationship was also recovered for 9 and 11–14 (data not shown). It reflects that the residual catalytic activity of a postulated ternary ESI complex depended on the concentration of the substrate.

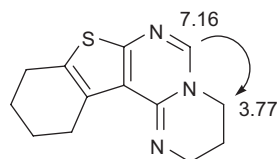


Figure 2. Relevant nuclear overhauser effect enhancement of compound 12. The spectrum was recorded in CDCl_3 .

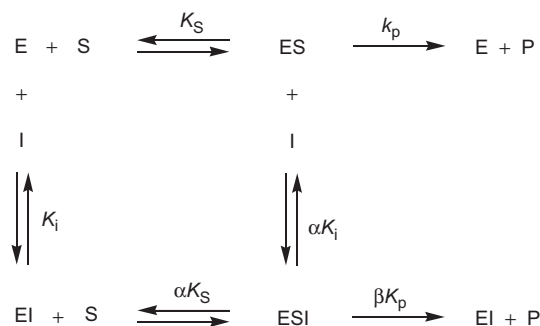


Figure 3. Kinetic model for the interaction of hyperbolic mixed-type inhibitors with *Electrophorus electricus* acetylcholinesterase. ES, enzyme-substrate complex; ESI, enzyme-substrate-inhibitor complex; EI, enzyme-inhibitor complex.

The parameters obtained by the kinetic analyses of the hyperbolic mixed-type inhibition of EeAChE by 9–14 are given in Table 1. These heterocyclic compounds inhibited EeAChE with K_i values of less than 3 μM . Most α values were relatively close to 1, indicating a similar affinity of the inhibitor to the free enzyme and the ES complex. Inhibitor 10 displayed a rather uncompetitive pattern of inhibition ($\alpha = 0.47$). Noteworthy, the highest β value was also obtained for 10, indicating that EeAChE when saturated with 10, would exhibit a relatively high residual activity. From the observed $v_{[I] \rightarrow \infty}$ values and the derived β values different from zero, the occurrence of a ternary ESI complex could be predicted (Figure 3). For 9–14, a purely competitive type of inhibition and thus a relevant interaction with the esteratic site of AChE could therefore be excluded.

Structure-activity relationships for the cholinesterase-inhibiting activity of 7–14 could be drawn as follows. Among the linearly fused derivatives 7–10, the presence of a basic *N*-benzyl moiety was a prerequisite for potency against EeAChE. Inhibitors 9 and 10 resembled donepezil, AP2238, and I (Figure 1) with respect to the benzyl substituent, its attachment to a basic nitrogen and the carbonyl group in a similar distance. The crystal structure of TcAChE complexed with donepezil²⁰ showed the inhibitor oriented along the axis of the gorge, extending from the anionic site to the PAS. Main interaction occurred through aromatic π - π stacking between Trp84 and the benzyl moiety of donepezil, orientated to the bottom of the gorge, and between Trp279 and the indanone ring of donepezil. The charged piperidine nitrogen made a cation- π interaction with Phe330 at the midpoint of the gorge. The carbonyl interacted with the aromatic rings of Phe331 and Phe290, and indirectly *via* a water molecule with the amide bond of Phe288. Donepezil did not directly interact with residues of the catalytic triad. Similar contacts stabilized the complex of AP2238 with human AChE as concluded from docking studies. The coumarin ring interacted with the PAS and the carbonyl group established an H-bond interaction with a phenylalanine backbone amide group²¹. Donepezil, AP2238 and I have been described as mixed-type inhibitors of EeAChE group^{21,22,34}. Moreover, 4*H*-pyrido[4',3':4,5]thieno[2,3-*d*][1,3]oxazin-4-ones, relatives of I, showed a reduced inhibitory potency towards EeAChE when the benzyl rest was shortened, whereas an exchange of *N*-benzyl by oxygen or a methylene unit led to a loss in activity¹⁹. The kinetic analyses, as discussed above, and the structural resemblance to the known inhibitors led us to suspect a similar orientation of our inhibitors 9 and 10 in the active-site gorge of AChE.

Compounds 7 and 8 were inactive against the human enzymes hAChE and hBChE, too, while the AChE-inhibiting activity of 9 and 10 was also observed at hAChE. Compound 9 was completely inactive against hBChE. Compound 10 was the most active representative of this series at hAChE with an IC_{50} of around 6 μM . It exhibited a 10-fold higher IC_{50} value at hBChE.

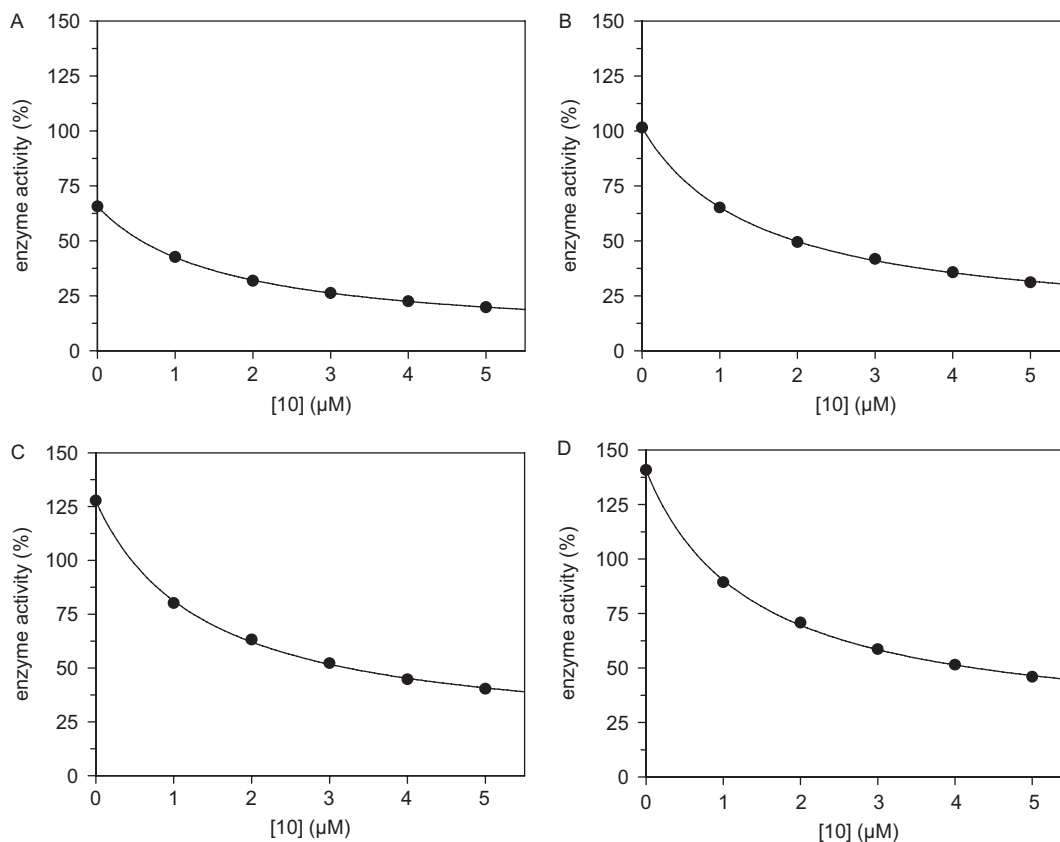


Figure 4. Inhibition of *Electrophorus electricus* acetylcholinesterase (EeAChE) by compound **10**. Plot of the rates versus $[I]$ for the inhibition of EeAChE in 100 mM sodium phosphate, 100 mM NaCl, pH 7.3 with 350 μM 5,5'-dithio-bis-(2-nitrobenzoic acid) (DTNB), 6% acetonitrile and $\sim 0.03\text{U/mL}$ EeAChE. Rates were obtained by linear regression of the progress curves and are mean values of duplicate experiments. A rate at a substrate concentration of 500 μM in the absence of inhibitor was set 100%. (A) Initial substrate concentration was 250 μM acetylthiocholine (ATCh). The solid line was drawn using the best-fit parameters from a fit according to Equation 1, which gave $\text{IC}_{50} = 1.61 \pm 0.04\ \mu\text{M}$ and $v_{[I] \rightarrow \infty} = 5.0 \pm 0.5\%$. (B) Initial substrate concentration was 500 μM ATCh. Non-linear regression according to Equation 1 gave $\text{IC}_{50} = 1.51 \pm 0.07\ \mu\text{M}$ (see Table 1) and $v_{[I] \rightarrow \infty} = 11 \pm 1\%$. (C) Initial substrate concentration was 750 μM ATCh. Non-linear regression according to Equation 1 gave $\text{IC}_{50} = 1.39 \pm 0.09\ \mu\text{M}$ and $v_{[I] \rightarrow \infty} = 17 \pm 2\%$. (D) Initial substrate concentration was 1000 μM ATCh. Non-linear regression according to Equation 1 gave $\text{IC}_{50} = 1.38 \pm 0.07\ \mu\text{M}$ and $v_{[I] \rightarrow \infty} = 20 \pm 2\%$.

Unexpectedly, the angularly fused heterocycles 11–14 were all found to inhibit EeAChE in the low micromolar range, regardless whether they possess a basic, benzyl-substituted nitrogen or not. Their α values were somewhat higher than 1, indicating a mixed-type inhibition with a slightly pronounced competitive character. These inhibitors, lacking the carbonyl group of the angular derivatives, might be accommodated in a different way along the active-site gorge. However, as they exhibited only weak potency against human AChE and no selectivity for hAChE over hBChE, a more detailed investigation was not attempted.

Conclusions

A series of eight tetracyclic compounds (7–14) was prepared by routes starting from 2-aminothiophene derivatives, accessible by Gewald reaction. The kinetic analysis of the hyperbolic mixed-type inhibition of EeAChE by 9–14 performed in this study was based on the determination of the inhibitory parameters K_i , αK_i , and β . A residual enzymatic activity at an infinite inhibitor concentration and thus a catalytically active ternary ESI complex was

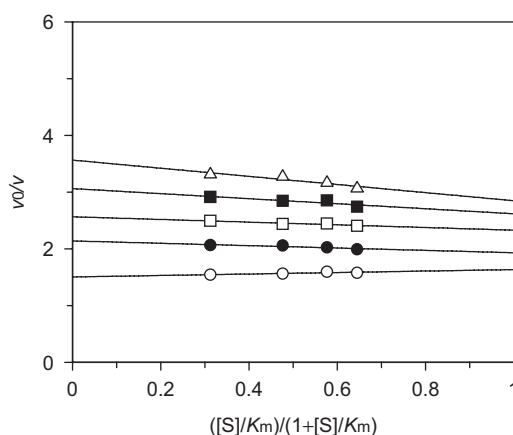


Figure 5. Specific velocity plot for the inhibition of *Electrophorus electricus* acetylcholinesterase (EeAChE) by compound **10**. Concentrations of **10** were as follows: open circles, $[I] = 1\ \mu\text{M}$; full circles, $[I] = 2\ \mu\text{M}$; open squares, $[I] = 3\ \mu\text{M}$; full squares, $[I] = 4\ \mu\text{M}$; open triangles, $[I] = 5\ \mu\text{M}$. Data were from duplicate measurements at four different substrate concentrations (250 μM , 500 μM , 750 μM , and 1000 μM). Linear regression according to Equation 2 gave values for vertical intercepts at $([S]/K_m)/(1+[S]/K_m) = 0$ (a values) and for vertical intercepts at $([S]/K_m)/(1+[S]/K_m) = 1$ (b values).

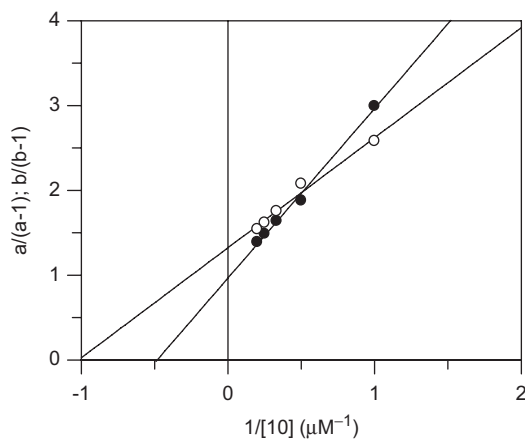


Figure 6. Replots of the specific velocity plot shown in Figure 5. Values $a/(a-1)$ (full circles) and $b/(b-1)$ (open circles) were plotted versus the reciprocal concentrations of inhibitor 10. Linear regression according to Equations 3 and 4 gave values $K_i = 2.07 \pm 0.19 \mu\text{M}$, $\alpha K_i = 0.98 \pm 0.13 \mu\text{M}$, $\beta = 0.24$.

concluded for the active compounds 9–14. These compounds do not reach the potency and selectivity of other cholinesterase inhibitors, in particular those of some tacrine-derived dimers. However, the linearly fused derivative 10, exhibiting an IC_{50} value of around $6 \mu\text{M}$ for human AChE, will serve as a starting point for further structural modifications. For example, an extrusion of the thiophene sulfur would result in a structure of higher flexibility and more closely related to that of donepezil, with an *N*-benzyl piperidine moiety as substituent at a bicyclic system.

Declaration of interest

This work was supported by the DFG, Graduate College 677.

References

- Soreq H, Seidman S. Acetylcholinesterase—new roles for an old actor. *Nat Rev Neurosci* 2001; 2:294–302.
- Silman I, Sussman JL. Acetylcholinesterase: ‘classical’ and ‘non-classical’ functions and pharmacology. *Curr Opin Pharmacol* 2005; 5:293–302.
- Sussman JL, Harel M, Frolow F, Oefner C, Goldman A, Toker L, Silman I. Atomic structure of acetylcholinesterase from *Torpedo californica*: a prototypic acetylcholine-binding protein. *Science* 1991; 253:872–879.
- Colletier JP, Fournier D, Greenblatt HM, Stojan J, Sussman JL, Zaccai G, Silman I, Weik M. Structural insights into substrate traffic and inhibition in acetylcholinesterase. *EMBO J* 2006; 25:2746–2756.
- Johnson G, Moore SW. The peripheral anionic site of acetylcholinesterase: structure, functions and potential role in rational drug design. *Curr Pharm Des* 2006; 12:217–225.
- Inestrosa NC, Dinamarca MC, Alvarez A. Amyloid-cholinesterase interactions. Implications for Alzheimer’s disease. *FEBS J* 2008; 275:625–632.
- Giacobini E, Becker RE. One hundred years after the discovery of Alzheimer’s disease. A turning point for therapy? *J Alzheimers Dis* 2007; 12:37–52.

- Melnikova I. Therapies for Alzheimer’s disease. *Nat Rev Drug Discov* 2007; 6:341–342.
- Muñoz-Torrero D, Camps P. Dimeric and hybrid anti-Alzheimer drug candidates. *Curr Med Chem* 2006; 13:399–422.
- Musial A, Bajda M, Malawska B. Recent developments in cholinesterases inhibitors for Alzheimer’s disease treatment. *Curr Med Chem* 2007; 14:2654–2679.
- Muñoz-Torrero D. Acetylcholinesterase inhibitors as disease-modifying therapies for Alzheimer’s disease. *Curr Med Chem* 2008; 15:2433–2455.
- Lin G, Liu YC, Lin YF, Wu YG. Ortho effects in quantitative structure-activity relationships for acetylcholinesterase inhibition by aryl carbamates. *J Enzyme Inhib Med Chem* 2004; 19:395–401.
- Marco-Contelles J, León R, de Los Ríos C, Guglietta A, Terencio J, López MG, García AG, Villarroya M. Novel multipotent tacrine-dihydropyridine hybrids with improved acetylcholinesterase inhibitory and neuroprotective activities as potential drugs for the treatment of Alzheimer’s disease. *J Med Chem* 2006; 49:7607–7610.
- Elsinghorst PW, Tanarro CM, Gütschow M. Novel heterobivalent tacrine derivatives as cholinesterase inhibitors with notable selectivity toward butyrylcholinesterase. *J Med Chem* 2006; 49:7540–7544.
- Tumiatti V, Minarini A, Bolognesi ML, Milelli A, Rosini M, Melchiorre C. Tacrine derivatives and Alzheimer’s disease. *Curr Med Chem* 2010; 17:1825–1838.
- Elsinghorst PW, Cieslik JS, Mohr K, Tränkle C, Gütschow M. First gallamine-tacrine hybrid: design and characterization at cholinesterases and the M2 muscarinic receptor. *J Med Chem* 2007; 50:5685–5695.
- Elsinghorst PW, Härtig W, Goldhammer S, Grosche J, Gütschow M. A gorge-spanning, high-affinity cholinesterase inhibitor to explore beta-amyloid plaques. *Org Biomol Chem* 2009; 7:3940–3946.
- Härtig W, Kacza J, Paulke BR, Grosche J, Bauer U, Hoffmann A, Elsinghorst PW, Gütschow M. *In vivo* labelling of hippocampal beta-amyloid in triple-transgenic mice with a fluorescent acetylcholinesterase inhibitor released from nanoparticles. *Eur J Neurosci* 2010; 31:99–109.
- Pietsch M, Gütschow M. Synthesis of tricyclic 1,3-oxazin-4-ones and kinetic analysis of cholesterol esterase and acetylcholinesterase inhibition. *J Med Chem* 2005; 48:8270–8288.
- Kryger G, Silman I, Sussman JL. Structure of acetylcholinesterase complexed with E2020 (Aricept): implications for the design of new anti-Alzheimer drugs. *Struct Fold Des* 1999; 7:297–307.
- Piazzi L, Rampa A, Bisi A, Gobbi S, Belluti F, Cavalli A, Bartolini M, Andrisano V, Valenti P, Recanatini M. 3-(4-[[Benzyl(methyl)amino]methyl]phenyl)-6,7-dimethoxy-2H-2-chromenone (AP2238) inhibits both acetylcholinesterase and acetylcholinesterase-induced beta-amyloid aggregation: a dual function lead for Alzheimer’s disease therapy. *J Med Chem* 2003; 46:2279–2282.
- Pietsch M, Christian L, Inhester T, Petzold S, Gütschow M. Kinetics of inhibition of acetylcholinesterase in the presence of acetonitrile. *FEBS J* 2009; 276:2292–2307.
- Ram VJ, Pandey HK, Vlietinck AJ. Thieno[2,3-d]pyrimidines as potential chemotherapeutic agents. II. *J Heterocyclic Chem* 1981; 18:1277–1280.
- Smolanka IV, Khripak SM, Frolova NP, Dobosh AA. Alkylation of 2-thioureido-3-carboxythiophenes. *Ukr Khim Zh* 1979; 45:871–872.
- Leistner S, Gütschow M, Wagner G. The facile synthesis of 2-aminothieno[2,3-d][1,3]thiazin-4-ones, in some cases 5,6-anellated. *Synthesis* 1987; 466–470.
- Leistner S, Wagner G, Gütschow M, Glusa E. Synthesis of 7-benzyl-5,6,7,8-tetrahydro-pyrido[4’,3’:4,5]thieno [2,3-d]pyrimidine-4(3H)-ones with alkylthioester groups in position 2 and examination of their platelet aggregation-inhibiting activity. *Pharmazie* 1986; 41:54–55.

27. Leistner S, Gütschow M, Vieweg H, Wagner G, Strohscheidt T, Grupe R. Various synthetic routes to imidazo[1,2-c]thieno[3,2-e]pyrimidines and pyrimido[1,2-c]thieno[3,2-e]pyrimidines in some cases anellated. *Pharmazie* 1988; 43:756-760.
28. Ghorab MM. New biologically active N-(tetrahydrobenzothienopyrimidin-4-yl)-amino acids, thiourethane, sulfonamides and related compounds. *Phosphorus Sulfur Silicon Relat Elem* 2000;165:221-35.
29. Ellman GL, Courtney KD, Andres V, Feather-Stone RM. A new and rapid colorimetric determination of acetylcholinesterase activity. *Biochem Pharmacol* 1961;7:88-95.
30. Huang Y, Dömling A. The Gewald multicomponent reaction. *Mol Divers* 2010 (DOI: 10.1007/s11030-010-9229-6).
31. Leistner S, Gütschow M, Wagner G. A facile synthesis of 2-alkylthio-4-amino-thieno[2,3-d]pyrimidines. *Arch Pharm (Weinheim)* 1989;322:227-30.
32. Segel IH. *Enzyme kinetics. Behavior and analysis of rapid equilibrium and steady-state enzyme systems.* New York: John Wiley & Sons Inc., 1993:161-226.
33. Baici A. The specific velocity plot. A graphical method for determining inhibition parameters for both linear and hyperbolic enzyme inhibitors. *Eur J Biochem* 1981; 119:9-14.
34. Nochi S, Asakawa N, Sato T. Kinetic study on the inhibition of acetylcholinesterase by 1-benzyl-4-[(5,6-dimethoxy-1-indanon)-2-yl]methylpiperidine hydrochloride (E2020). *Biol Pharm Bull* 1995; 18:1145-1147.